

A Macrocyclic Tetradentate Complex. Structure of 1,4,8,11-Tetrathiacyclotetradecanenickel(II) Tetrafluoroborate, Ni(TTP)(BF₄)₂, and Electron Paramagnetic Resonance Spectra of Its ⁶³Cu-Doped Crystals

P. H. DAVIS, L. K. WHITE, and R. L. BELFORD*

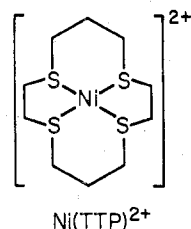
Received November 5, 1974

AIC40765U

The crystal and molecular structure of 1,4,8,11-tetrathiacyclotetradecanenickel(II) tetrafluoroborate, Ni(TTP)(BF₄)₂, has been determined from three-dimensional X-ray data collected on an automatic diffractometer using Mo K α radiation. The red-brown crystals belong to space group $P2_1/c$ with $a = 9.603$ (6) Å, $b = 9.029$ (5) Å, $c = 11.451$ (5) Å, $\beta = 110.86$ (4)°, and $Z = 2$. The structure was solved by standard methods and refined to a residual $R = 0.050$. The NiS₄ moiety is a nearly perfect square plane; all the S–Ni–S bond angles are $90 \pm 0.3^\circ$ and the Ni–S bond distances are 2.176 ± 0.002 Å. However, the five- and six-membered rings involving the Ni and S atoms have a pleated conformation. The EPR parameters for a ⁶³Cu-doped single crystal are as follows: $g_{\parallel} = 2.087$, $g_{\perp} = 2.026$, $A_{\parallel} = 0.0172$ cm⁻¹, $A_{\perp} = 0.0045$ cm⁻¹. Despite the strong aplanarity of the rings, the g_{\parallel} direction is approximately perpendicular to the local chelate (CuS₄) plane, and the g and A tensors are coincident. In some orientations, all 16 γ -hydrogen nuclei display an approximately equal superhyperfine splitting of 2–3 G.

Introduction

As part of a continuing study in this laboratory of bonding and electronic structure in complexes of copper(II), and in particular of square-planar complexes with sulfur donor ligands, we have had occasion to investigate the electron paramagnetic resonance spectra of single crystals of 1,4,8,11-tetrathiacyclotetradecanenickel(II) tetrafluoroborate, Ni(TTP)(BF₄)₂, in which a portion of the nickel(II) had been



isomorphously replaced by copper(II). Our primary aim was to determine the ⁶³Cu nuclear quadrupole coupling parameters in aid of a general correlation of copper(II) electronic and molecular structures with coupling constants. The conventional EPR study and determination of the X-ray structure of the host lattice, carried out in preparation for the quadrupole study, showed interesting features of their own and are reported here.

In addition to the current general interest in complexes involving multidentate macrocyclic ligands which may mimic sites occurring in nature, the crystal and molecular structures of Ni(TTP)(BF₄)₂ are of interest in their own right because of the opportunity afforded for comparison with the recently characterized structures of related complexes of the nitrogen donor ligand 1,4,8,11-tetraazacyclotetradecane (cyclam),^{1,2} as well as with the structures of the widely studied nickel(II) dithiolate complexes.³ While a resistance to displacement reactions has been noted in the case of the cyclam complex,⁴ Busch and Rosen⁵ have reported an unusual reactivity of the nickel–sulfur complex with nucleophiles of moderate donor strength, e.g., H₂O and DMSO. Significant structural differences from the dithiolate complexes might be expected due to the geometrical constraints of the macrocyclic ligand.

Experimental Section

1,4,8,11-Tetrathiacyclotetradecanenickel(II) Tetrafluoroborate. The ligand and complex were prepared as described by Busch and Rosen.⁵ Ni(TTP)(BF₄)₂ was doped with ⁶³Cu for the EPR studies in the following manner. A 0.5-mg sample of ⁶³CuO (obtained from Isotope Sales Division, Oak Ridge National Laboratory) was dissolved in concentrated hydrochloric acid and the solution evaporated to dryness. The residue and 0.25 g of Ni(TTP)(BF₄)₂ were dissolved in nitro-

ethane and suitable single crystals grown by slow evaporation.

Anal. Calcd for C₁₀H₂₀S₄NiB₂F₈: C, 23.98; H, 4.02; Ni, 11.73; S, 25.61. Found: C, 24.09; H, 3.98; Ni, 11.83; S, 25.69.

Crystal Data: C₁₀H₂₀S₄Ni(BF₄)₂, mol wt 500.9, monoclinic ($P2_1/c$), $a = 9.603$ (6) Å, $b = 9.029$ (5) Å, $c = 11.451$ (5) Å, $\beta = 110.86$ (4)°, $V = 927.8$ Å³, ρ_{measd} (floatation in carbon tetrabromide and carbon tetrachloride at 25°) = 1.76 g cm⁻³, $Z = 2$, $\rho_{\text{calcd}} = 1.80$ g cm⁻³, $F(000) = 508$, $\mu(\text{Mo K}\alpha) = 15.55$ cm⁻¹.

X-Ray Data Collection and Reduction. Preliminary precession (Mo K α) and Weissenberg (Cu K α) photographs showed Laue symmetry $2/m$. Systematic absences $h0l$ for $l = 2n + 1$ and $0k0$ for $k = 2n + 1$ unambiguously determine the space group as $P2_1/c$.

The crystal chosen for data collection measured $0.45 \times 0.35 \times 0.25$ mm and was mounted with the b crystallographic axis coincident with the spindle (ϕ) axis. All data were collected on a Picker FACS-I automated diffractometer equipped with scintillation counter and pulse height analyzer. Unit cell parameters were obtained from a least-squares fit to the angular settings of ten reflections with $2\theta \geq 45^\circ$ which had been centered on the Mo K α_1 peak, λ 0.70930 Å. Intensities were measured by a moving-crystal, moving-counter scan technique (zirconium-filtered Mo K α radiation with λ 0.7107 Å). A basic scan width of 2° (2θ) was used, to which was added a dispersion factor to take into account the K α_1 –K α_2 splitting. Reflections were scanned at a rate of $1^\circ/\text{min}$, 10-sec stationary background counts being taken at the low- and high-angle extremes of each scan. Calibrated copper foil attenuators were automatically inserted into the diffracted beam whenever the counting rate exceeded 10,000 counts/sec. Three standard reflections from diverse regions of reciprocal space were measured after every 75 reflections to monitor crystal and electronic stability. Following a power outage midway through data collection, the intensities of the standard reflections decreased by 3.5%. (This same factor was obtained by taking the mean value of the intensity ratios for an overlapping set of 50 reflections measured when data collection resumed.) Within the two sets of data (before and after the outage) plots of the intensities of the standard reflections showed no discernible trend and all intensities were within $\pm 1.3\%$ of their mean value. Therefore, a single scale factor was applied to the data collected following the power outage and no other scaling was done.

The raw data were corrected for background, for Lorentz and polarization effects, and for the use of attenuators. Both because absorption should not substantially affect atom positions⁶ and because we estimated it to affect no F_0 by more than $\pm 6\%$ for our crystal, we made no absorption corrections. An estimated standard deviation in the intensity of each reflection was calculated from the formula

$$\sigma(I) = [C + (t_c/2t_b)^2(B_1 + B_2) + (pN)^2]^{1/2}$$

where C is the total integrated peak count obtained in a scan time t_c , B_1 and B_2 are the background counts at each end of the scan, each obtained in a time t_b , and the term in N , the net count, is included to take into account deviations from sources other than counting statistics.^{7,8} The parameter p was assigned a value of 0.03. Of the

Table I. Final Positional and Thermal Parameters for $C_{10}H_{20}S_4Ni(BF_4)_2^a$

	x/a	y/b	z/c	β_{11}	β_{22}	β_{33}	β_{12}	β_{13}	β_{23}
Ni	0.0000 ^b	0.5000 ^b	0.5000 ^b	0.0074 (1)	0.0075 (1)	0.0043 (1)	0.0000 (1)	0.0019 (1)	-0.0001 (1)
S1	0.0819 (1)	0.3839 (1)	0.3706 (1)	0.0097 (1)	0.0078 (1)	0.0057 (1)	-0.0002 (1)	0.0033 (1)	-0.0006 (1)
S2	0.1617 (1)	0.3843 (1)	0.6565 (1)	0.0087 (1)	0.0082 (1)	0.0052 (1)	0.0003 (1)	0.0014 (1)	0.0005 (1)
C1	0.2775 (6)	0.4273 (7)	0.4160 (5)	0.0105 (7)	0.0138 (9)	0.0096 (6)	-0.0012 (6)	0.0056 (5)	-0.0010 (5)
C2	0.3657 (5)	0.3541 (6)	0.5399 (5)	0.0090 (6)	0.0113 (7)	0.0115 (6)	0.0006 (5)	0.0039 (5)	-0.0003 (5)
C3	0.3444 (5)	0.4227 (7)	0.6536 (5)	0.0080 (6)	0.0134 (8)	0.0082 (5)	0.0003 (6)	0.0011 (4)	-0.0001 (5)
C4	0.1599 (5)	0.4894 (6)	0.7903 (4)	0.0131 (7)	0.0105 (6)	0.0049 (3)	-0.0009 (6)	0.0012 (4)	-0.0001 (4)
C5	0.0006 (6)	0.5126 (6)	0.7742 (4)	0.0161 (7)	0.0130 (7)	0.0054 (4)	-0.0002 (7)	0.0048 (4)	-0.0002 (5)
B	0.2828 (6)	0.6608 (7)	0.0963 (5)	0.0116 (7)	0.0127 (8)	0.0065 (5)	0.0014 (6)	0.0025 (5)	-0.0006 (5)
F1	0.2623 (5)	0.5123 (4)	0.0881 (3)	0.0392 (10)	0.0110 (5)	0.0137 (4)	0.0013 (5)	0.0107 (5)	-0.0017 (3)
F2	0.4087 (4)	0.6998 (5)	0.0784 (4)	0.0171 (6)	0.0390 (10)	0.0169 (5)	0.0019 (6)	0.0099 (5)	0.0090 (6)
F3	0.2931 (4)	0.7041 (4)	0.2145 (3)	0.0272 (7)	0.0177 (5)	0.0098 (3)	-0.0019 (5)	0.0080 (4)	-0.0038 (3)
F4	0.1681 (4)	0.7319 (4)	0.0090 (3)	0.0192 (6)	0.0209 (6)	0.0136 (4)	0.0077 (5)	-0.0016 (4)	-0.0014 (4)

	x/a	y/b	z/c	$B, \text{\AA}^2$		x/a	y/b	z/c	$B, \text{\AA}^2$
H11	0.293 (7)	0.394 (7)	0.355 (6)	6.6 (1.6)	H32	0.351 (6)	0.525 (6)	0.649 (5)	5.0 (1.3)
H12	0.281 (5)	0.533 (5)	0.413 (4)	3.2 (1.0)	H41	0.212 (5)	0.586 (5)	0.795 (4)	3.1 (0.9)
H21	0.356 (5)	0.250 (6)	0.542 (4)	4.6 (1.2)	H42	0.220 (5)	0.440 (5)	0.863 (5)	4.0 (1.0)
H22	0.477 (5)	0.361 (5)	0.547 (4)	3.5 (0.9)	H51	-0.004 (6)	0.571 (6)	0.837 (5)	4.9 (1.2)
H31	0.419 (6)	0.388 (6)	0.724 (5)	5.2 (1.2)	H52	-0.066 (5)	0.404 (5)	0.759 (4)	3.7 (1.0)

^a The form of the anisotropic thermal parameter is $\exp[-(\beta_{11}h^2 + \beta_{22}k^2 + \beta_{33}l^2 + 2\beta_{12}hk + 2\beta_{13}hl + 2\beta_{23}kl)]$. Estimated standard deviations in the least significant digit(s) are given in parentheses here and in subsequent tables. See Figure 1 for the atom-labeling scheme. ^b Coordinates of the Ni atom fixed by symmetry.

2713 unique reflections with $2\theta \leq 60^\circ$, 842 had $I \leq 2\sigma(I)$ and were excluded from the refinement. (A structure factor calculation at the end of the refinement indicated that none of the reflections thus excluded should have had a net intensity greater than the minimum value which could consistently be observed as significantly above the background.)

Determination and Refinement of Structure.⁹ Solution and refinement of the structure proceeded by standard methods. An initial Patterson map revealed the positions of the two independent sulfur atoms. A Fourier map phased on the positions of the sulfur atoms and the nickel atom, whose position was fixed by symmetry considerations, served to locate four of the carbon atoms, while a second Fourier synthesis incorporating this additional information was sufficient to locate all remaining nonhydrogen atoms.

Full-matrix least-squares refinement was carried out on F . The function minimized was $\sum w(|F_o| - |F_c|)^2$, where $|F_o|$ and $|F_c|$ are the observed and calculated structure factor amplitudes, respectively, and the weight w assigned to each reflection was $4F_o^2/\sigma^2(F_o^2)$, $\sigma(F_o^2)$ being derived from $\sigma(I)$ above. Scattering curves for neutral Ni, S, F, C, and B were calculated from the analytical function and coefficients tabulated by Cromer and Mann.¹⁰ The hydrogen scattering curve was that of Stewart et al.¹¹ The effects of anomalous dispersion were taken into account in the structure factor calculations using values of $\Delta f'$ and $\Delta f''$ for Ni given in ref 12.

Refinement of a model including all nonhydrogen atoms with individual atom isotropic thermal parameters converged to $R_1 [= \sum |F_o| - |F_c| / \sum |F_o|] = 0.094$ and $R_2 [= (\sum w(|F_o| - |F_c|)^2 / \sum w|F_o|^2)^{1/2}] = 0.109$. Further refinement with individual atom anisotropic thermal parameters reduced the R factors to $R_1 = 0.061$ and $R_2 = 0.072$. A difference Fourier synthesis at this point clearly revealed the positions of all ten hydrogen atoms. Addition of the hydrogen atoms with individual atom isotropic thermal parameters to the model and subsequent refinement resulted in $R_1 = 0.052$ and $R_2 = 0.057$. Application of the simple statistical test suggested by Hamilton¹³ indicates that both the use of anisotropic thermal parameters for the nonhydrogen atoms and the inclusion of the hydrogen atoms in the model produce significant improvement at a 99.5% confidence level.

Examination of a listing of $|F_o|$ and $|F_c|$ at this point suggested that four low-order reflections (100, 120, -121, and 130) were suffering from extinction effects and they were given zero weight in the final refinement cycle. The refinement finally converged with $R_1 = 0.050$ and $R_2 = 0.055$. The standard deviation of an observation of unit weight was 1.97. During the final cycle of refinement no parameter changed by more than 0.25 of its estimated standard deviation. The maximum electron density in a final difference Fourier map was associated with the position of the Ni atom. Its magnitude, 1.2 e/\AA^3 , was approximately one-fifth of that of a typical carbon peak in a Fourier map at this point. Elsewhere in the difference map the maximum peak magnitude was 0.6 e/\AA^3 .

Final least-squares atomic parameters with estimated standard

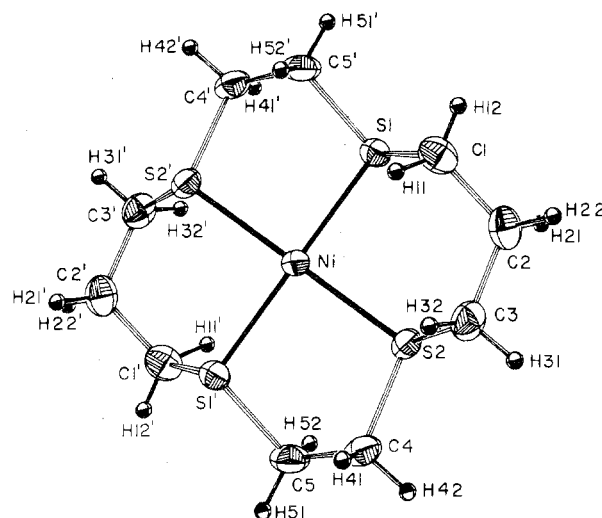


Figure 1. A perspective view of the $Ni(C_{10}H_{20}S_4)^{2+}$ ion normal to the NiS_4 plane, illustrating the square-planar coordination geometry and showing the atom-labeling scheme used (atoms denoted by primes are related to the corresponding unprimed atoms by inversion through the position of the Ni atom). Atoms are represented by 35% probability thermal ellipsoids.

deviations derived from the inverse matrix are given in Table I. A listing of observed and calculated structure factor amplitudes for all reflections used in the refinement is available.¹⁴

Spectra. X-Band EPR spectra were obtained on a Varian E-9 (9-GHz) spectrometer. The spectrometer frequency was monitored with a Hewlett-Packard digital frequency meter (Model 5240A) and dpph was used as a g marker.

The orientation of the crystal in the magnetic field was varied by use of a locally constructed goniometer¹⁵ which provides for rotation of the crystal about two mutually perpendicular axes. One rotation axis is coincident with the central vertical axis of the EPR cavity, the second being in the plane of the magnetic field. This design allows one to obtain all possible orientations of the crystal in the magnetic field from a single arbitrary crystal mounting.

Q-Band EPR spectra were obtained on a Varian E-15 (35-GHz) spectrometer. Crystals were mounted on paraffin wedges to obtain the desired orientations with respect to the magnetic field.

Results and Discussion

Description of Structure. The most noteworthy aspect of the structure of the $Ni(TTP)^{2+}$ ion, shown in Figure 1, is the high degree to which the NiS_4 coordination polyhedron ap-

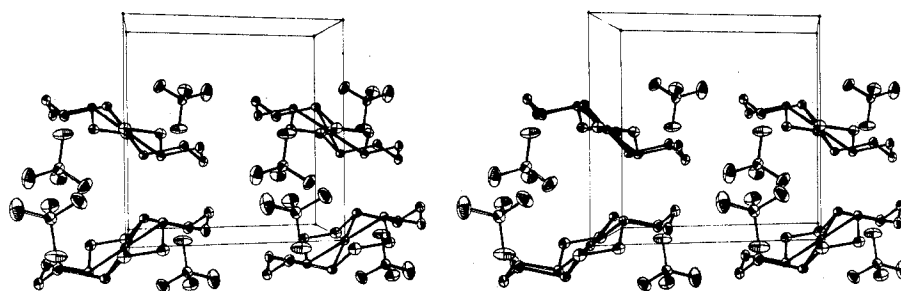


Figure 2. A stereoscopic view of the packing in Ni(C₁₀H₂₀S₄)(BF₄)₂. Note that NiS₄ planes of successive molecules are nearly perpendicular to one another. Atoms are represented by 35% probability thermal ellipsoids.

Table II. Summary of Important Interatomic Distances and Angles

a. Distances Å			
Ni-S1	2.177 (1)	S2-C3	1.800 (5)
Ni-S2	2.175 (1)	S2-C4	1.808 (5)
S1-C1	1.804 (6)	C1-C2	1.520 (8)
S1-C5'	1.821 (6)	C2-C3	1.519 (8)
		C4-C5	1.489 (8)
		B-F1	1.353 (7)
		B-F2	1.343 (7)
		B-F3	1.378 (7)
		B-F4	1.357 (7)
b. Angles, Deg			
S1-Ni-S2	90.25 (10)	C3-S2-C4	102.6 (2)
Ni-S1-C1	106.9 (2)	S1-C1-C2	110.6 (4)
Ni-S1-C5'	103.2 (2)	C1-C2-C3	115.0 (4)
Ni-S2-C3	107.9 (2)	C2-C3-S2	111.5 (3)
Ni-S2-C4	103.1 (2)	S2-C4-C5	106.8 (2)
C1-S1-C5'	102.8 (3)	C4-C5-S1'	106.2 (2)
		F1-B-F2	111.5 (4)
		F1-B-F3	107.9 (3)
		F1-B-F4	111.0 (5)
		F2-B-F3	108.8 (5)
		F2-B-F4	107.6 (3)
		F3-B-F4	110.1 (5)

proximates exact square-planar geometry (*D*_{4h} symmetry) even though the ligand ring itself is strongly pleated and twisted. Because the Ni atom is located at an inversion center, the five atoms are crystallographically constrained to be coplanar. In addition, although not required by symmetry to be so, the two independent Ni-S bonds are equal in length and the S-Ni-S angle is 90° to within experimental uncertainty. The important interatomic distances and angles are summarized in Table II (not included in the table are the ten C-H distances (average 0.961 Å, rms deviation 0.088 Å) and 25 H-C-H and C-C-H angles (average 109°, rms deviation 5°)).

The EPR data suggested that the NiS₄ planes of the two molecules in the unit cell were approximately perpendicular to one another, a fact which was confirmed by the X-ray structure (see Figure 2). From the crystallographic data the angle between the normals to the two planes was found to be 94.1°. (In an orthogonal coordinate system in which the *y* axis is taken to be coincident with the crystallographic *b* axis and the *z* axis normal to the *ab* plane, the equation of the NiS₄ plane determined by the atoms whose coordinates are listed in Table I is 0.6758*X* + 0.7319*Y* + 0.0874*Z* - 2.3940 = 0.)

Comparison to Related Structures. A large number of 1,1- and 1,2-dithiolate complexes containing square-planar NiS₄ have been characterized crystallographically.³ In by far the majority of these structures the Ni was found, as in the present case, to be located at a site of inversion symmetry requiring the Ni and S atoms to be rigorously coplanar. In the 1,1-dithiolate complexes a four-member chelate ring is formed. The small "bite" of the chelating ligand results in significant distortions from square geometry, the average intrachelate S-Ni-S angle being 79°. However, in the 1,2-dithiolate complexes with five-member chelate rings the average intrachelate S-Ni-S angle is 91° and in several complexes the angle is exactly 90° to within the experimental uncertainty. The Ni-S distance of 2.176 Å observed in the present case is midway between the 2.101-2.166 Å range observed for the 1,2-dithiolates and the 2.19-2.24 Å range for the 1,1-dithiolates. That this bond in Ni(TTP)²⁺ is shorter than in the 1,1-dithiolate complexes is probably largely due to the larger chelate ring in the present case which can accommodate the shorter length without undue ring strain, while the difference from the 1,2-dithiolate complexes is probably an electronic

Table III. Comparison of Some Average Interatomic Distances and Angles in Complexes Containing Square-Planar NiS₄

	Ni-S, Å	C-S, Å	S-Ni-S, deg	S-C-X, deg
1,1-Dithiolates ^a	2.22 ± 0.03	1.70 ± 0.03	79 ± 2	111 ± 3
1,2-Dithiolates ^a	2.14 ± 0.03	1.73 ± 0.03	91 ± 2	119 ± 3
Ni(TTP) ²⁺ ^b	2.18	1.81	90	109

^a Reference 3. ^b This work.

effect associated with the fact that 1,4,8,11-tetrathiacyclotetradecane is saturated while the dithiolate ligands are unsaturated. The difference between saturated and unsaturated ligands is also manifested in the length of the C-S bond and the bond angle at the α carbon (see Table III). The C-S distance is about average for a saturated C-S bond.¹⁶ One further noteworthy difference between the present complex and the bulk of the dithiolate complexes is the fact that in Ni(TTP)²⁺ the ligand itself is not coplanar with the NiS₄ grouping.

Complexes of nickel(II) with cyclam, an amine analog of TTP, and its N-methylated derivative have also been characterized crystallographically.^{1,2} The basic configuration of the ligand skeleton is the same in all three complexes, the six-membered chelate rings having a chair conformation and the two-carbon residues being twisted out of the coordination plane (see Figure 2). The 14-membered heterocyclic rings may be described as distorted seven-pointed crowns. Deviations from 90° of the bond angles around Ni are significantly larger in the amine complexes. It should be noted that both of the amine complexes were octahedral, the axial coordination sites being occupied in the one case by chloride ions and in the other by bridging azide ions. The present complex is most certainly four-coordinate. The Ni-B distance is 6.31 Å, while the minimum Ni-F distance is 5.34 Å (the distance from Ni to the surface of a sphere centered on B and enclosing the entire BF₄⁻ ion is 4.93 Å). This may be compared to the observed range of 2.12-2.56 Å in cases of confirmed BF₄⁻ coordination.¹⁷ The two independent S-Ni-B angles are 42.1 and 110.3°.

EPR Results. Rotation of the magnetic field in two mutually perpendicular crystal planes revealed two magnetically inequivalent but chemically equivalent ⁶³Cu sites, with the typical

Table IV. Electronic Zeeman and Hyperfine Interaction Parameters for Some Four-Coordinate Copper(II) Thio Chelates

Ref	Chelate ^a	g_{\parallel}	g_{\perp}	$ A_{\parallel} ^b$	$ A_{\perp} $	$\langle A \rangle$	$ A_{\parallel} - A_{\perp} $
This paper	Cu(TTP) ²⁺ powder ^c	2.088	2.027	172	48	89	124
This paper	⁶³ Cu(TTP) ²⁺ crystal ^c	2.087	2.026	172	45	87	127
18, 19	Cu(MNT) ₂ ²⁻ ^c	2.086	2.026	162	39	80	123
			2.025			(76) ^e	
20	Cu(DTC) ₂ ^c	2.084	2.020	159	36	79	120
			2.023		42	(59) ^d	

^a MNT = dithiomaleonitrile, SC(CN)C(CN)S²⁻; DTC = diethyldithiocarbamate, (C₂H₅)₂NCS₂⁻. ^b All hyperfine coupling constants (A) are given in units of 10^{-4} cm⁻¹. ^c In the corresponding Ni host. ^d In the corresponding Zn host. The site symmetry here allows direct Cu(d_{xy})-Cu(s) mixing, which can strongly influence the hyperfine contact interaction. See ref 20. ^e EPR data for Cu(MNT)₂²⁻ solutions.

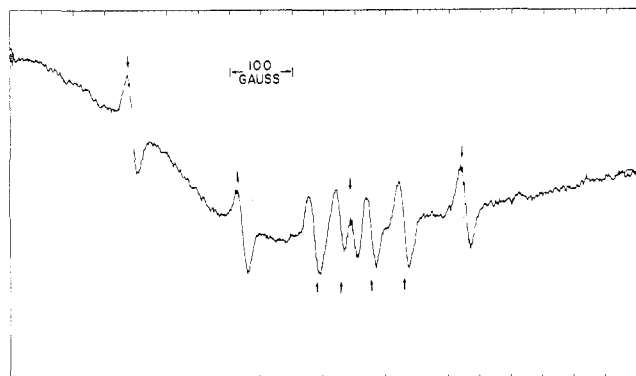


Figure 3. X-Band EPR spectrum of a ⁶³Cu-doped single crystal of Ni(TTP)(BF₄)₂ at lowest field orientation for one magnetic site (i.e., g_{\parallel} , A_{\parallel}). Arrows above the base line point out the parallel resonances; arrows below the base line point out resonances belonging to the other magnetic site. The rolling base line is an artifact of the goniometer. Magnetic field increases from left to right.

two sets of four principal line groups coalescing to one set in at least one direction in each plane, and suggested the $P2_1/c$ space group which was subsequently confirmed in the X-ray study. Within the experimental limits, we determined the Zeeman (g) and ⁶³Cu hyperfine (A) tensors to be coincident (to within $\pm 1^\circ$) and essentially axial. Through successive angular adjustments a crystal plane was located such that when one line set occurred at its absolute minimum resonance field position (g_{\parallel} , A_{\parallel}), the other set was approximately at its maximum (g_{\perp} , A_{\perp}); see Figure 3. Rotation of $90 \pm 3^\circ$ in this plane produced an identical spectrum. Since the structural study (vide supra) revealed the angle between the chelate (NiS₄) planes of the host molecules to be 94° , we infer that the guest and host molecules have very nearly the same orientation of their chelate planes and that the g and A tensor axes are effectively determined by the CuS₄ chelate planes.

The g and A values obtained from the single crystal are consistent with these inferred from EPR spectra of powders containing naturally occurring ⁶³Cu and ⁶⁵Cu; see Figures 3 and 4 and Table IV.

Orientation of Zeeman Axes. The rough coincidence of the principal axes of the g tensor with those of both the A tensor and the CuS₄ plane is particularly interesting. Because the C-S bonds are directed well out of the MS₄ plane (see Figure 1), one might expect the available sulfur orbitals which could interact with the Cu orbitals to be strongly skewed out of the axis system of the chelate plane. As a result, interaction between these ligand orbitals and the metal orbitals could cause the g_{\parallel} direction to be substantially shifted away from the normal to the CuS₄ plane. Any such effect would appear to be small in this case.

Zeeman and Copper Hyperfine Parameters. Table IV lists the anisotropic g and A values for some complexes having the CuS₄ grouping.¹⁸⁻²⁰ The g parameters are essentially the same for all. The deviations of g_{\parallel} and g_{\perp} from the free-electron values are smaller than in the corresponding compounds with

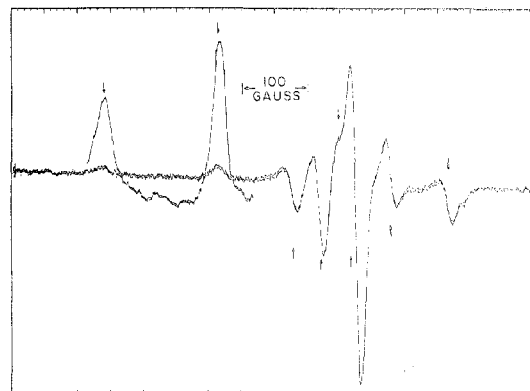


Figure 4. X-Band EPR spectrum of a powder of Ni(TTP)(BF₄)₂ doped with Cu in natural abundance. Arrows above the base line point out parallel resonances (g_{\parallel} , A_{\parallel}); arrows below the base line, perpendicular ones (g_{\perp} , A_{\perp}). Magnetic field increases from left to right.

oxygen donor ligands, suggesting more covalent copper-ligand primary (σ - δ) bonds, substantial contributions of ligand (S) spin-orbit coupling, smaller effective charge on the copper ion (causing lower effective metal spin-orbit coupling), and/or greater ligand field splittings. The copper hyperfine interaction is also quite similar for all these complexes with sulfur donors. The contact term ($\langle A \rangle = (A_{\parallel} + 2A_{\perp})/3$; we assume A_{\parallel} and A_{\perp} to have the same sign), $(84 \pm 5) \times 10^{-4}$ cm⁻¹, shows a little variation among the complexes. The fact that it is about the same as in the four-coordinate planar Cu(II) complexes with oxygen ligands ($\sim 75 \times 10^{-4}$ cm⁻¹) means that the electron spin density at the Cu nucleus does not vary greatly even though the principal part of the spin density (in an antibonding orbital involving d_{xy}) should be considerably more delocalized in the thio complexes. Evidently such delocalization is compensated by an increased effectiveness of spin polarization of the copper s-electron density. The hyperfine anisotropy ($|A_{\parallel}| - |A_{\perp}|$) is nearly the same, ~ 0.0123 cm⁻¹, for all of these thio complexes and is about 20% less than the hyperfine anisotropy in four-coordinate planar copper complexes with oxygen ligands (typically ~ 0.0155 cm⁻¹).²¹ This reduction is entirely consistent with the greater spin delocalization in the thio complexes.

Superhyperfine Structure. Line widths in the EPR spectra of planar CuS₄ complexes are usually narrow, ~ 1 -2 G. EPR line widths for the ⁶³Cu-Ni(TTP)²⁺ system are much broader, ~ 20 G; the greater breadth is caused by superhyperfine structure. Figure 5 shows a Q-band EPR spectrum of one of the ⁶³Cu hyperfine lines at the parallel orientation. The observed intensity pattern matches reasonably well with the 17-line intensity pattern for 16 equivalent or nearly equivalent hydrogens (1:16:120:560:1820:4368:8008:11,440:12,870...). Presumably, the 16 nearly equivalent hydrogens are those at the γ positions, i.e., located on the 1, 1', 3, 3', 4, 4', 5, and 5' carbon atoms (see Figure 1). The superhyperfine splitting is 2-3 G and a slight broadening of the superhyperfine structure toward the wings of each line group could indicate some small

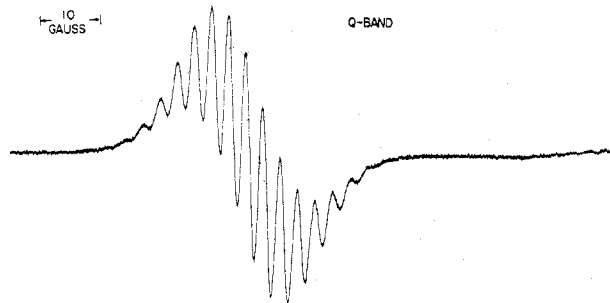


Figure 5. Q-Band EPR spectrum of a ^{63}Cu -doped single crystal of $\text{Ni}(\text{TTP})(\text{BF}_4)_2$ for one of the ^{63}Cu hyperfine lines at the parallel orientation showing superhyperfine structure. Magnetic field increases from left to right.

inequivalencies among the hydrogens. Superhyperfine structure can be seen at other orientations, but it is less well resolved. The effect may indicate greater magnetic inequivalencies among the hydrogens at these orientations. Although the general magnitude of the superhyperfine coupling is not surprising, the near equivalence of all the γ hydrogens is noteworthy. Evidently, in the $\text{Cu}(\text{TTP})^{2+}$ complex the spin density is spread out onto the carbon skeleton in an especially uniform way.

Acknowledgment. We thank the donors of the Petroleum Research Fund, administered by the American Chemical Society, for support of this research. We also thank Professors E. Kent Barefield and Iain C. Paul for valuable contributions and discussions.

Registry No. $\text{Ni}(\text{TTP})(\text{BF}_4)_2$, 25460-51-9; ^{63}Cu , 14191-84-5.

Supplementary Material Available. A listing of structure factor amplitudes will appear following these pages in the microfilm edition of this volume of the journal. Photocopies of the supplementary material from this paper only or microfiche (105 \times 148 mm 24 \times reduction, negatives) containing all of the supplementary material for papers in this issue may be obtained from the Journals Department,

American Chemical Society, 1155 16th St., N.W., Washington, D.C. 20036. Remit check or money order for \$4.50 for photocopy or \$2.50 for microfiche, referring to code number AIC40765U.

References and Notes

- B. Bosnich, R. Mason, P. J. Pauling, G. B. Robertson, and M. L. Tobe, *Chem. Commun.*, 97 (1965).
- (a) N. F. Curtis, D. A. Swann, and T. N. Waters, *J. Chem. Soc., Dalton Trans.*, 19, 1963 (1973); (b) F. Wagner, M. T. Mocella, J. D'Aniello, Jr., A. H.-J. Wang, and E. K. Barefield, *J. Am. Chem. Soc.*, 96, 2625 (1974).
- For a review of structural studies of nickel(II)-dithiolate complexes prior to 1969 see R. Eisenberg, *Prog. Inorg. Chem.*, 12, 295 (1970). More recent studies include G. P. Khare, A. J. Schultz, and R. Eisenberg, *J. Am. Chem. Soc.*, 93, 3597 (1971); J. M. Martin, P. W. G. Newman, B. W. Robinson, and A. H. White, *J. Chem. Soc., Dalton Trans.*, 20, 2233 (1972); P. W. G. Newman and A. H. White, *ibid.*, 20, 2239 (1972).
- B. Bosnich, M. L. Tobe, and G. A. Webb, *Inorg. Chem.*, 4, 1109 (1965).
- D. H. Busch and W. Rosen, *J. Am. Chem. Soc.*, 91, 4694 (1969).
- R. C. Srivastava and E. C. Lingafelter, *Acta Crystallogr.*, 20, 918 (1966).
- W. R. Busing and H. A. Levy, *J. Chem. Phys.*, 26, 563 (1957).
- P. W. R. Corfield, R. Doedens, and J. A. Ibers, *Inorg. Chem.*, 6, 197 (1967).
- Programs for the IBM 360/75 used in this analysis were local modifications of Rodgers and Johnson's ALF Fourier program, Busing, Martin, and Levy's ORFLS least-squares refinement program, and Johnson's ORTEP thermal ellipsoid plotter program.
- D. T. Cromer and J. B. Mann, *Acta Crystallogr., Sect. A*, 24, 321 (1968).
- R. F. Stewart, E. R. Davidson, and W. T. Simpson, *J. Chem. Phys.*, 42, 3175 (1965).
- "International Tables for X-Ray Crystallography", Vol. III, Kynoch Press, Birmingham, England, 1962, p 215.
- W. C. Hamilton, *Acta Crystallogr.*, 18, 502 (1965).
- Supplementary material.
- Design kindly provided by Dr. J. R. Pilbrow, Physics Department, Monash University, Clayton, Victoria, Australia 3168.
- Chem. Soc., Spec. Publ.*, No. 18, S22s (1965).
- A. P. Gaughan, Jr., Z. Dori, and J. A. Ibers, *Inorg. Chem.*, 13, 1657 (1974).
- A. H. Maki, N. Edelstein, A. Davidson, and R. H. Holm, *J. Am. Chem. Soc.*, 86, 4580 (1964).
- E. Billig, R. Williams, I. Bernal, J. H. Waters, and H. B. Gray, *Inorg. Chem.*, 3, 663 (1964).
- M. J. Weeks and J. P. Fackler, *Inorg. Chem.*, 7, 2548 (1968).
- (a) A. H. Maki and B. R. McGarvey, *J. Chem. Phys.*, 29, 31 (1958); (b) B. R. McGarvey, *Transition Met. Chem.*, 3, 160 (1966); (c) M. A. Hitchman and R. L. Belford in "ESR of Metal Complexes", Teh Fu Yen, Ed., Plenum Press, New York, N.Y., 1969, p 97.

Contribution from the Department of Chemistry, University of Alabama, University, Alabama 35486, from the Laboratoire de chimie de coordination, Paris 5 $^{\circ}$, France, and from the Department of Chemistry, University of Massachusetts, Amherst, Massachusetts 01002

Molecular Structures of the Bis(η^5 -indenyl)dimethyl Derivatives of Titanium, Zirconium, and Hafnium

JERRY L. ATWOOD,*^{1a} WILLIAM E. HUNTER,^{1a} DUANE C. HRNCIR,^{1a} EDMOND SAMUEL,^{1b} HELMUT ALT,^{1c} and MARVIN D. RAUSCH*^{1c}

Received November 19, 1974

AIC40796P

The crystal structures of the series $(\eta^5\text{-C}_9\text{H}_7)_2\text{M}(\text{CH}_3)_2$, where M = Ti, Zr, and Hf, have been determined from three-dimensional X-ray data measured by counter methods. The compounds are isostructural and crystallize in the orthorhombic space group $P2_12_12$ [D_{2h}^3 ; No. 18]. For bis(η^5 -indenyl)dimethyltitanium(IV) the unit cell dimensions are $a = 14.124$ (7) Å, $b = 8.073$ (5) Å, $c = 6.844$ (5) Å, and $Z = 2$. Full-matrix least-squares refinement has led to a final R value of 0.070 based on 280 independent observed reflections. For bis(η^5 -indenyl)dimethylzirconium(IV) the cell dimensions are $a = 14.248$ (4) Å, $b = 8.244$ (3) Å, and $c = 6.929$ (3) Å. The refinement led to a final R value of 0.025 based on 904 reflections. For bis(η^5 -indenyl)dimethylhafnium(IV) the cell dimensions are $a = 14.243$ (6) Å, $b = 8.215$ (4) Å, and $c = 6.918$ (4) Å. The refinement led to a final R value of 0.031 based on 965 reflections. The effect of the lanthanide contraction is evident even with the cell parameters: that of hafnium has a volume of 5 Å³ less than that of zirconium. The molecules have crystallographically imposed twofold symmetry. In each case the metal-carbon σ -bond length is 0.2–0.3 Å shorter than the metal-carbon distances for the η^5 ligands. Although the Hf-C(η^5) approach (2.53 Å average) is closer than with the Zr analog (2.55 Å average), the Hf-C(σ) length (2.332 (12) Å) is significantly longer than the Zr-C(σ) distance (2.251 (6) Å). The values for the titanium complex are Ti-C(η^5) = 2.44 Å (average) and Ti-C(σ) = 2.21 (2) Å.

Introduction

The organometallic chemistry of titanium has been rather extensively developed over the past two decades, while that of zirconium and hafnium is only now beginning to emerge. Structural studies have done much to elucidate the nature of

the titanium-carbon bond in compounds which contain ligands coordinated in a polyhaptic fashion.^{2–10} Likewise, the geometry of several cyclopentadienylzirconium compounds has been established: $(\eta^5\text{-C}_5\text{H}_5)_2\text{ZrF}_2$,¹¹ $(\eta^5\text{-C}_5\text{H}_5)_2\text{ZrCl}_2$,¹² $(\text{CH}_2)_3(\eta^5\text{-C}_5\text{H}_4)_2\text{ZrCl}_2$,¹³ $(\eta^5\text{-C}_5\text{H}_5)_2\text{ZrI}_2$,¹¹ $(\eta^5\text{-C}_5\text{H}_5)$ -